

Cosmic Mass Spectrometer

Luis A. Anchordoqui,^{1,2,3} Vernon Barger,⁴ and Thomas J. Weiler⁵

¹Department of Physics & Astronomy, Lehman College, City University of New York, NY 10468, USA

²Department of Physics, Graduate Center, City University of New York, NY 10016, USA

³Department of Astrophysics, American Museum of Natural History, NY 10024, USA

⁴Department of Physics, University of Wisconsin, Madison, WI 53706, USA

⁵Department of Physics & Astronomy, Vanderbilt University, Nashville, TN 37235, USA

We argue that if ultrahigh-energy ($E \gtrsim 10^{10}$ GeV) cosmic rays are heavy nuclei (as indicated by existing data), then the pointing of cosmic rays to their nearest extragalactic sources is expected for $10^{10.6} \lesssim E/\text{GeV} \lesssim 10^{11}$. This is because for a nucleus of charge Ze and baryon number A , the bending of the cosmic ray decreases as Z/E with rising energy, so that pointing to nearby sources becomes possible in this particular energy range. In addition, the maximum energy of acceleration capability of the sources grows linearly in Z , while the energy loss per distance traveled decreases with increasing A . Each of these two points tend to favor heavy nuclei at the highest energies. The traditional bi-dimensional analyses, which simultaneously reproduce Auger data on the spectrum and nuclear composition, may not be capable of incorporating the relative importance of all these phenomena. In this paper we propose a multi-dimensional reconstruction of the individual emission spectra (in E , direction, and cross-correlation with nearby putative sources) to study the hypothesis that primaries are heavy nuclei subject to GZK photo-disintegration, and to determine the nature of the extragalactic sources. More specifically, we propose to combine information on nuclear composition and arrival direction to associate a potential clustering of events with a 3-dimensional position in the sky. Actually, both the source distance and maximum emission energy can be obtained through a multi-parameter likelihood analysis to accommodate the observed nuclear composition of each individual event in the cluster. We show that one can track the level of GZK interactions on an statistical basis by comparing the maximum energy at the source of each cluster. We also show that nucleus-emitting-sources exhibit a *cepa stratis* structure on Earth which could be peeled off by future space-missions, such as POEMMA. Finally, we demonstrate that metal-rich starburst galaxies are highly-plausible candidate sources, and we use them as an explicit example of our proposed multi-dimensional analysis.

I. INTRODUCTION

The most important result so far from the present generation of ultrahigh-energy cosmic ray (UHECR) observatories is the conclusive evidence that the cosmic ray (CR) flux drops precipitously for energies beyond $E \approx 10^{10.6}$ GeV. The discovery of this suppression was first reported by the HiRes [1] and Auger collaborations [2], and later confirmed by the Telescope Array (TA) [3].¹ By now (in Auger data) the suppression has reached a statistical significance of more than 20σ [5].

There are two competing classes of models to explain the observed suppression. The competing models are the Greisen, Zatsepin, and Kuz'min (GZK) effect due to the CR interaction with the cosmic microwave background (CMB) [6, 7], and the *disappointing* model [8] wherein it is postulated that the “end-of steam” for cosmic accelerators is coincidentally near the putative GZK cutoff, with the exact energy cutoff determined by data. Since both models accommodate the same rate in the mean, it is a challenge to discriminate between them.

In this paper we re-examine the GZK interactions in the nearby universe (where the models differ most) and discuss a method that can be used to discriminate be-

tween the two classes of models. Indeed, model discrimination becomes feasible by analyzing UHECR events beyond the onset of the suppression. Throughout we will refer to these events as trans-GZK events. We show that when information on nuclear composition is combined with the distribution of arrival directions it is possible to elaborate a concrete mapping of clustered trans-GZK events, which can isolate the source location in 3-dimensions. To positively associate a potential cluster with a 3-dimensional position in the sky, we need information on the nuclear composition of each event in the cluster. This is because each nuclear species exhibits different propagation characteristics, which arrange a natural *mass spectrometer* in the local (distance $\lesssim 50$ Mpc) universe. At the same time, we can determine the maximum CR energy of the source producing the cluster, which together with the propagation distance controls the level of GZK interactions. As an illustrative example, we invoke starburst galaxies as the sources of UHECRs.

GZK noted that the extragalactic UHECR flux could be dominated either by protons or nuclei, with the GZK effect driven by photo-pion production and photo-disintegration, respectively [6, 7]. For heavy nuclei, photo-disintegration on the cosmic infrared (IR) background is also relevant in modeling the high-energy tail of the spectrum [9]. If UHECRs are protons then there is only one *visible* effect of the GZK interactions, which is the suppression of the spectrum around $10^{10.6}$ GeV. However, as we advanced above and demonstrate be-

¹ Evidence for a suppression in the spectrum, from data of first generation UHECR experiments, was pointed out in [4].

low, if UHECR are nuclei there is more to observe than just the suppression of the spectrum.

The atmospheric depth at which the longitudinal development of a CR shower has its maximum, X_{\max} , and the number of muons N_{μ} reaching ground level are the most powerful observables to determine the UHECR nuclear composition [10]. The Auger high-quality, high-statistics data, when interpreted with existing hadronic event generators, exhibit a strong likelihood for a composition that becomes gradually heavier with increasing energy, beginning around $10^{9.7}$ GeV [11–15]. Within uncertainties, the data from TA are consistent with these findings [16, 17].

In addition, TA has observed a statistically significant excess in cosmic rays with energies above 57 EeV in a region of the sky spanning about 20° , centered on equatorial coordinates R.A. = 146.7° , Dec. = 43.2° [18]. This is colloquially referred to as the “TA hot spot.” The chance probability of this hot spot in an isotropic CR sky was calculated to be $p_{\text{TA}} = 3.7 \times 10^{-4}$ (3.4σ) [19]. The absence of a concentration of nearby sources in this region of the sky corroborates other experimental evidence for UHECR nuclei, in that a few local sources within the GZK sphere can produce the hot spot through significant deflection and translation (proportional to the nucleus charge Ze) in the extragalactic and Galactic magnetic fields. More recently, this picture has been further supported by Auger data, which revealed an intermediate-scale anisotropy, with statistical significance of 4σ [20, 21].²

If the highest-energy primary CRs are dominated by heavy nuclei, there are important implications for the astrophysics of the sources. For example, a trend toward heavier composition could reflect the endpoint of cosmic acceleration. The acceleration of primaries is proportional to Z , so heavy nuclei can be expected to dominate the composition near the end of the spectrum (with E_{\max} coincidentally falling off near the expected GZK cutoff region [8]). In such a model, the suppression would constitute an imprint of the accelerator characteristics rather than energy loss in transit. Such a model has been termed the *disappointing* model [8], in that no physics beyond acceleration in sources is invoked.Suppressions due to source end points and due to GZK losses are simultaneously possible.

The general idea behind our method of discrimination is summarized in the following axioms (the first two arising from the GZK effect):

- The higher the energy the heavier the nuclear species.
- The higher the energy the smaller the number of apparent sources, because nuclei lose energy

roughly proportional to their distance of travel, thus favoring the few nearby sources.

- The higher the energy of a cosmic ray proton the smaller the bending on the magnetic field and therefore the smaller the angle between the incident CR direction at Earth and the line-of-sight to the true source.
- The higher the energy of a cosmic ray nuclei the bending decreases as Z/E .

The collection of spectral and anisotropic features and nuclear composition observables undoubtedly reflect physically interesting phenomena, including source distribution(s), emission properties, and propagation effects.

A common approach to interpreting spectral features and nuclear composition is to develop some hypothesis about source properties and, using either analytic or Monte Carlo methods, to predict the mean spectrum and the average nuclear composition expected at Earth. As our knowledge of source distributions and properties is limited, it is common practice to assume spatially homogeneous and isotropic UHECR emissions. A mean spectrum and average nuclear composition are then computed, based on this assumption. If, following Auger and TA data, the composition is taken to be mixed, then the simultaneous fit to the spectrum and composition (e.g., X_{\max} distribution) imposes severe constraints on model parameters: (i) hard source spectra and (ii) “low” energy cutoff, of order $10^{9.7} Z$ GeV [22–24]. We note in passing that the constraint on the spectral index can be relaxed by considering a negative source evolution with redshift [25], but the assumption of softer source spectra leaves the energy cutoff unaltered (see e.g. Fig. 11 in [23]). Now, a robust argument can be advanced: for the source parameters given above, it is extremely challenging to distinguish between the two classes of models. The rationale will be given by example. At first sight it will appear that if a substantial fraction of the trans-GZK events are oxygen or lighter nuclei, then GZK interactions must be at play, as the source maximum energy for oxygen would be $10^{10.6}$ GeV. However, we note that the earthly maximum energy for an oxygen nucleus which is produced as a surviving fragment of a heavier nucleus during propagation is roughly the same; say, for an iron nucleus the source maximum energy would be $E_{\max} \sim 10^{11.2}$ GeV, and so after losing 40 nucleons the energy of the oxygen would also be close to $10^{10.6}$ GeV. This would make the two classes of models almost indistinguishable.

The line of argumentation given above is of course limited to the assumption of an homogeneous source distribution. In reality this assumption cannot be correct, especially at the highest energies where the GZK effect severely limits the number of sources visible to us. We can quantify the possible deviation from the mean prediction based on the knowledge we do have on the

² Throughout “intermediate” denotes angular scales larger than the angular resolution of the Auger array, which is about 1° , and smaller than large-scale patterns, i.e., below about 45° .

source density and the pointing distances to the closest source populations. This fluctuation about the mean has been referred to as the ensemble fluctuation [26]. The local fluctuations will present their strongest effect for the most energetic cosmic rays, due to the limited propagation distance in the cosmic radiation background (see e.g. Fig. 2 in [27]). In other words, the strongest effect is a local phenomenon, unique to our local Galactic geometry, and a manifestation of the *cosmic variance*.

As shown in [28], the UHECR flux of sources beyond 100 Mpc can be well approximated by a homogeneous distribution of sources. However, the finite (non-zero) distance to the nearest source of UHECR nuclei leads to a breakdown of the homogeneous source distribution spectrum result at the highest energies. The combined fit to the spectrum and X_{\max} distribution considering a non-zero distance to the first source leads to a maximum injection energy in the range $10^{11.5} < E_{\max}/\text{GeV} < 10^{12}$, depending on the nuclear species. We arrive then at the fifth axiom of our method of discrimination:

- The discreteness of nearby UHECR emitters must be considered.

Putting all this together we come up with a new analysis technique to discriminate between the two classes of models. Namely, we propose to combine information on nuclear composition and arrival direction to associate a potential clustering of trans-GZK events with a 3-dimensional position in the sky. For a given cluster, the distance to the source is determined through a multi-parameter fit to the observed nuclear composition of each individual event, in conjunction with possible GZK energy losses. Model discrimination can be done on an statistical basis by comparing the best fit parameters of each individual cluster.³

The rest of the paper is organized as follows. In Sec. II we re-examine the interactions of UHECR nuclei on the pervasive sea of microwave and infrared radiation filling the universe. We show that, for $10^{10.5} \lesssim E/\text{GeV} \lesssim 10^{11.5}$ and propagation distances $\lesssim 50$ Mpc, a fully analytic treatment of the energy losses that UHECR nuclei suffer *en route* to Earth becomes feasible. This is because the effects of pair and photo-meson production can be safely neglected and we need to only consider a single energy loss mechanism: photo-disintegration. Most importantly, we point out that we can use information on the nuclear composition to pin down the origin of any potential cluster of trans-GZK events appearing in the distribution of arrival directions. We also comment on the experimental sensitivity of such analysis for existing

and future UHECR observatories. In Sec. III we confront the information on magnetic field deflections contained in our third and fourth axioms to develop a new method to discriminate between accelerators of UHECR protons and sources of UHECR nuclei. In Sec. IV we particularize our discussion to starburst galaxies. We first revise a two-step acceleration model presented elsewhere [30] to accommodate the new needs of source spectra that can reproduce Auger data. After that we derive accurate predictions for the earthly nuclear composition that can be confronted with experimental data on an event-by-event basis. We show that existing data are consistent with the characteristics of nucleus-emitting-sources delineated in Sec. III. The paper wraps up with some conclusions presented in Sec. V.

II. ENERGY LOSS AS A TRACE OF SOURCE DISTANCE

The relevant mechanisms for the GZK energy loss that extremely high-energy nuclei are expected to suffer on the way to Earth are: pair production in the field of the nucleus, photo-disintegration, and meson photo-production. In the nucleus rest-frame, pair production has a threshold at ~ 1 MeV, photo-disintegration is particularly important at the peak of the giant dipole resonance (GDR) that corresponds to photon energies of 15 to 25 MeV, and photo-meson production has a threshold energy of ~ 145 MeV.⁴ For $10^{10.5} \lesssim E/\text{GeV} \lesssim 10^{11.5}$ and propagation distances $\lesssim 50$ Mpc, the effect of pair and photo-meson production can be safely neglected [31], i.e. at the high-energy end of the heavy-nuclei spectrum, the photo-disintegration process dominates the energy losses.⁵ With this dominance, we now exploit a complete analytic treatment of the GZK effect.

The interaction time τ_A^{int} for a highly relativistic nucleus with energy $E = \gamma A m_p$ (where γ is the Lorentz factor) propagating through an isotropic photon background with energy ε and spectrum $dn(\varepsilon)/d\varepsilon$, is [34]

$$\frac{1}{\tau_{\text{int}}} = \frac{c}{2} \int_0^\infty \frac{1}{\gamma^2 \varepsilon^2} \frac{dn(\varepsilon)}{d\varepsilon} d\varepsilon \int_0^{2\gamma\varepsilon} \varepsilon' \sigma_A(\varepsilon') d\varepsilon', \quad (1)$$

where $\sigma_A(\varepsilon')$ is the cross section for photo-disintegration of a nucleus with baryon number A by a photon of energy ε' in the rest frame of the nucleus. We have found that

³ It is noteworthy that the actual observation of the GZK effect would provide strong constraints on Lorentz invariant breaking effects. This is because if Lorentz invariance is broken in the form of non-standard dispersion relations, then absorption and energy loss processes for UHECR interactions would be modified. See e.g. [29] for interactions of UHECR protons with the CMB.

⁴ For photo-disintegration, the averaged fractional energy loss equals the fractional loss in baryon number of the nucleus. During the photo-disintegration process the Lorentz factor of the nucleus is conserved, unlike the cases of pair production and photo-meson production processes, which involve the creation of new particles that carry off energy.

⁵ The inelasticity of (e^+e^-) pair production is very low ($\approx m_e/m_p$, for $Z = 1$) so that the energy loss of UHECRs is gradual. The characteristic lifetime for energy loss for this process at energies $\gtrsim 10^{10}$ GeV is $\tau = E/(dE/dt) \approx 5 \times 10^9$ yr [32]. For a nucleus, the energy loss rate is Z^2/A times higher than for a proton of the same Lorentz factor [33].

for the considerations in the present work, the GDR can be safely approximated by the single pole of the narrow-width approximation,

$$\sigma_A(\varepsilon') = \pi \sigma_0 \frac{\Gamma}{2} \delta(\varepsilon' - \varepsilon_0), \quad (2)$$

where $\sigma_0 = 1.45 \times 10^{-27} A \text{ cm}^2$, $\Gamma = 8 \times 10^6 \text{ eV}$, and $\varepsilon_0 = 42.65 \times 10^6 A^{-0.21} (9.25 \times 10^5 A^{2.433}) \text{ eV}$, for $A > 4$ ($A \leq 4$) [35]. The factor of 1/2 is introduced to match the integral (i.e. total cross section) of the Breit-Wigner and the delta function. Inserting (2) into (1) we obtain

$$\frac{1}{\tau_{\text{int}}} \approx \frac{c \pi \sigma_0 \varepsilon_0 \Gamma}{4\gamma^2} \int_{\varepsilon_0/2\gamma}^{\infty} \frac{d\varepsilon}{\varepsilon^2} \frac{dn(\varepsilon)}{d\varepsilon}. \quad (3)$$

For the CMB,

$$\frac{dn(\varepsilon)}{d\varepsilon} = \frac{1}{(\hbar c)^3} \left(\frac{\varepsilon}{\pi} \right)^2 [e^{\varepsilon/T} - 1]^{-1}, \quad (4)$$

and so (3) becomes [36]

$$\frac{1}{\tau_{\text{int}}^{\text{CMB}}} \approx \frac{1}{\hbar^3 c^2} \frac{\sigma_0 \varepsilon_0 \Gamma T}{4\gamma^2 \pi} \left| \ln(1 - e^{-\varepsilon_0/2\gamma T}) \right|, \quad (5)$$

with $T = 2.3 \times 10^{-4} \text{ eV}$. Following [37], we parametrize the spectral density of the cosmic IR background as,

$$\frac{dn(\varepsilon)}{d\varepsilon} \simeq 1.1 \times 10^{-4} \left(\frac{\varepsilon}{\text{eV}} \right)^{-2.5} \text{ cm}^{-3} \text{ eV}^{-1}, \quad (6)$$

where $2 \times 10^{-3} < \varepsilon/\text{eV} < 0.8$. For $\gamma \gtrsim 10^9$, the interaction time of a nucleus scattering off the IR is found to be

$$\frac{1}{\tau_{\text{int}}^{\text{IR}}} \approx 8 \times 10^{-6} \left(\frac{\sigma_0}{\text{cm}^2} \right) \left(\frac{\Gamma}{\text{eV}} \right) \left(\frac{\varepsilon_0}{\text{eV}} \right)^{-2.5} \gamma^{1.5} \text{ s}^{-1}. \quad (7)$$

Using numerical integration we have verified that, in the energy range of interest, different parametrizations of the cosmic IR background [38, 39] modify the interaction time scale given in (7) by $\lesssim 20\%$.

Our conclusions are encapsulated in Fig. 1, where we show the mean free path of UHECR nuclei scattering off the pervasive cosmic radiation fields. One sees that the interaction mean free path (mfp) decreases rapidly with increasing energy, and increases rapidly with increasing nuclear composition:

- at $E = 10^{10.6} \text{ GeV}$, the mfp for ionized helium (^4He) is about 3 Mpc, while at $10^{10.85} \text{ GeV}$ it is nil;
- at $E = 10^{11} \text{ GeV}$, the mfp for ionized oxygen (^{16}O) is about 4 Mpc, while at $10^{11.2} \text{ GeV}$ it is nil;
- It $E = 10^{11.2} \text{ GeV}$, the mfp for ionized silicon (^{28}Si) is about 2.5 Mpc, while at $10^{11.3} \text{ GeV}$ it is nil;
- etcetera, until finally we reach ionized iron (^{56}Fe) where the mfp at $E = 10^{11.3} \text{ GeV}$ is about 4 Mpc, while at $10^{10.44} \text{ GeV}$ it too is nil.

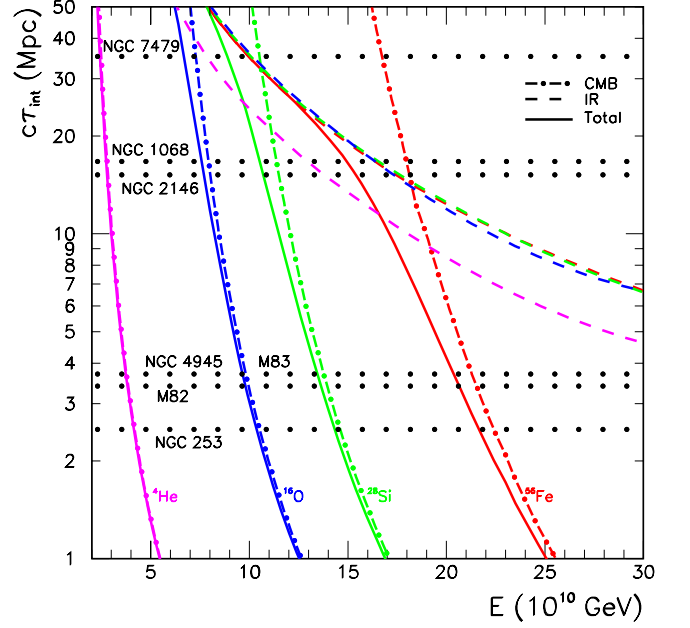


FIG. 1: Photo-disintegration mean free path on the CMB and IR photon fields for various nuclear species. The horizontal dotted lines indicate the distance to nearby starburst galaxies in the *Fermi*-LAT catalog [40], with flux emission (or upper limit) in the gamma ray band $0.1 < E/\text{GeV} < 100$ bigger than $5 \times 10^{-9} \text{ cm}^{-2} \text{ s}^{-1}$. Starburst galaxies provide the example of UHECR emitters which we employ.

Thus, we have a *cosmic mass spectrometer*. From sources at increasing distance, fewer and heavier nuclei at highest energies are expected to reach Earth. The main features in the energy evolution of the abundance of various nuclear species on Earth can be summarized as follows:

- the contribution of ^4He should decrease with rising energy and then essentially disappear above about $10^{10.7} \text{ GeV}$;
- on average, only species heavier than ^{16}O can contribute to the observed flux on Earth above 10^{11} GeV , with nuclear species lighter than ^{28}Si highly suppressed at $10^{11.6} \text{ GeV}$;
- the mean flux of iron nuclei becomes suppressed somewhat below $10^{11.4} \text{ GeV}$. This is the maximum average energy expected on Earth, and is in agreement at the 1σ level with Fly's Eye observations [41].

The three considerations enumerated above are similar to those obtained assuming a continuous source distribution, with cutoff at about 3 Mpc [42–44]. However, the GZK energy losses follow a trend with increasing energy similar to that expected for acceleration capability of the sources, which grows linearly in the charge Ze of the nucleus. Namely, as the sources start to run out of power, the contribution to the emission spectrum of light and intermediate mass nuclei should decrease as

the energy increases. Thus, additional information on the abundance of the different nuclear species on Earth from other nearby sources would be needed in order to distinguish between the two scenarios. Such additional information is provided by considering the discreteness of UHECR emitters.

The fractional energy loss per collision decreases with increasing baryon number, and so we expect large fluctuations over the mean at the highest energies. Moreover, one should expect additional background from residual nuclear fragments created by the propagation of heavy nuclei from very distant sources. However, our concluding remarks could be verified by analyzing the distribution of arrival directions, because *for a given CR with charged Ze, the higher the energy the smaller the bending, and therefore, the smaller the angle between the incident CR and the true source.*

Strictly speaking, for any potential cluster of trans-GZK events appearing in the distribution of arrival directions we can use the information on the nuclear composition of each independent event to determine the distance to the source of the cluster through a multi-parameter likelihood analysis. The set of free source parameters involved in the data analysis, containing all the relevant guidelines to vary the incident flux and information on the nuclear composition, are: (i) the flux normalization, (ii) the spectral index of the power-law fit, (iii) the maximum energy, (iv) the admixture of nuclear species, and (v) the distance (more precisely, the time of flight). The fit is constrained by propagation effects. The critical task of deriving a unique analytic relation for the likelihood function \mathcal{L} between the observed and emitted nuclear species becomes workable, because energy losses are entirely dominated by photo-disintegration. By the maximization of \mathcal{L} in terms of the free parameters we can estimate the most likely value for those parameters. The most likely value of the source distance can then be combined with the distribution of arrival direction in the cluster to search for possible correlation with source catalogs in 3-dimensions. Discrimination between the two classes of models can be done on an statistical basis by comparing the best parameter values, particularly the maximum energy at the source of each individual cluster.

Before proceeding, we pause to note an essential difference between the method proposed herein and the traditional technique used to search for the degree of correlation between the arrival directions of UHECRs and source catalogs. On the one hand, in standard cross-correlation analyses one has to impose a selection criteria on potential sources to select a subsample of the catalog which corresponds to a given class of objects. Moreover, usually one has to impose very selective cuts on source parameters to select the most powerful objects in the catalog. On the other hand, in the analysis proposed herein we first conduct a search for the distance to the origin of a given potential cluster through the multi-parameter likelihood analysis, and so all source parameters are fit

to the data. One can then search for cross-correlations with catalogs in 3-dimensions and so there is no need for selection of a particular class of sources. Our method will automatically search for all sources of UHECRs independently of their various possible *origins*.

We now turn to discuss the sensitivity of this analysis for existing and future UHECR observatories. Determination of the source distance with extremely high precision requires UHECR measurements with a large exposure and first-rate X_{\max} resolution (defined as the rms of the distribution $X_{\max}^{\text{reconstructed}} - X_{\max}^{\text{true}}$). For example, discrimination between light and heavy nuclei requires an X_{\max} resolution of about 50 g/cm^2 , whereas the discrimination between medium mass and heavy nuclei requires about 20 g/cm^2 [24]. For AugerPrime, the X_{\max} resolution ranges from 15 g/cm^2 for fluorescence detection to about 50 g/cm^2 for measurements of the surface detector array [45]. Note that because of the $\approx 15\%$ duty cycle of fluorescence facilities only a subsample of Auger events would have X_{\max} measurements with 15 g/cm^2 resolution. When information on X_{\max} is combined with measurements of N_{μ} and the muon shower maximum X_{\max}^{μ} , the resolution of the Auger surface detector can be significantly improved to about 40 g/cm^2 at 10^{10} GeV , reaching $\sim 25 \text{ g/cm}^2$ at 10^{11} GeV [45]. The Probe Of Extreme Multi-Messenger Astrophysics (POEMMA) is being designed to achieve orders-of-magnitude increase in statistics of observed UHECRs beyond $10^{10.6} \text{ GeV}$ [46]. POEMMA stereo observations will have a large enough sample of well reconstructed UHECR events, with a resolution of at least $\sim 60 \text{ g/cm}^2$. This will be enough to distinguish protons from heavy nuclei. At this point we should note that results of air shower simulations show that shower-to-shower fluctuations in X_{\max} are large, and even extreme compositions like pure proton and pure iron have a considerable overlap in their X_{\max} -distributions. This introduces a theoretical systematic uncertainty in the proposed likelihood analysis. We look forward to the nuclear composition being presented for each event [47], so that the analysis proposed in this paper can be undertaken.

III. CEPA STRATIS

Hitherto we have adopted a pragmatic approach and avoided the details of theoretical modeling of magnetic deflections. Magnetic fields are not well constrained by current data, but if we adopt recent models of the Galactic magnetic field [48–51], typical values of the deflections of UHECRs crossing the Galaxy are $\sim 10^\circ$ for $E/Z = 10^{10} \text{ GeV}$, depending on the direction consid-

ered [52–54].⁶

When the average magnetic field deflection is combined with the energy losses shown in Fig. 1, we can conclude that:

- Granting that the extragalactic UHECR population seem to include a significant fraction of nuclei we still expect to observe an anisotropy, due to the anisotropic distribution of matter within the GZK horizon.
- In particular, for $10^{10.6} \lesssim E/\text{GeV} \lesssim 10^{11}$, we expect to observed excesses in $\sim 15^\circ$ regions of the sky centered at nearby sources, associated with nuclei of $Z \lesssim 10$.
- For $E \gtrsim 10^{11}$ GeV, the population of UHECR nuclei observed at Earth must consist mostly of baryons with $Z \gtrsim 10$, or else protons. This statement can be verified by inspection of Fig. 1. Nuclei heavier than neon would suffer too much of a deflection to be contained in a $\sim 15^\circ$ hot spot, and in some cases (e.g. iron nuclei) may completely camouflage the exact location of the sources.
- The *cepa stratis* structure inherent to the search of nucleus-emitting-sources is in sharp contrast to the quest for UHECR proton accelerators, in which the higher the energy of the proton the smaller the bending on the magnetic field and therefore the smaller the angle between the incident proton direction at Earth and the line-of-sight to the true source. The future POEMMA mission, which is expected to monitor the full sky with an extremely-fast, highly-pixelized, immensely-large aperture, will become the optimal instrument to identify the various types of UHECR sources.
- The potential observation of hot spots from nearby sources with onion layers that increase in size with rising energy, or else the observation of compact hot spots that become denser, compressed, and increase the significance level at $E \gtrsim 10^{11}$ GeV could provide a determination of the UHECR nuclear composition. Such UHECR species determination would be completely independent of CR air shower properties, and consequently not affected by the large systematic uncertainties introduced by models of hadronic interactions at ultrahigh energies.

In closing, we stress that the *cepa stratis* structure originates in the peculiar balance of magnetic field deflections and energy losses of UHECR nuclei. As a consequence, this is a global effect. Whether a particular source of

UHECR nuclei could be exposed through its onion layers would depend on the direction considered in the sky.

All source types are represented within the GZK horizon for heavy nuclei, so all source types are *a priori* candidates for the nearby exploration. However, starburst galaxies are perhaps the leading candidate for UHECR nucleus-emitting sources, and so we will take them as the example for our study. Readers not so interested in the details of the starburst galaxies example which we develop next, can skip to the summary section.

IV. SOURCE EXAMPLE: STARBURST GALAXIES

It has long been suspected that galaxies with bursts of massive star formation (starbursts) have the power to accelerate UHECR nuclei [30, 56]. It has also been noted that the arrival directions of the highest energy cosmic rays recorded by the Fly’s Eye [41], AGASA [57, 58], and Yakutsk [59] experiments can be traced back to the two nearest starbursts: M82 and NGC 253 [60].

Starburst galaxies feature strong infrared emission by dust associated with high levels of interstellar extinction, strong UV spectra from the Lyman- α emission of hot OB stars, and considerable radio emission produced by recent supernova remnants. The luminosity of the Balmer lines, primarily H α and H β , gives a measure of the star formation rate. The central regions of starburst galaxies can be orders of magnitude brighter than those of normal spiral galaxies. From such an active region, it is known [61, 62] that a galactic-scale superwind is driven by the collective effect of supernovae and winds from massive stars. The high supernovae rate creates a cavity of hot gas ($\sim 10^8$ K) whose cooling time is much greater than the expansion time scale [63–66]. Since the wind is sufficiently powerful, it can blow out of the interstellar medium of the galaxy as a hot bubble. As the cavity expands a strong shock front is formed on the contact surface with the cool interstellar medium. Shock interactions with low and high density clouds produce X-ray continuum and optical line emission, respectively. This model is supported by numerical simulations, an example of which is shown in Fig. 2. The majority of nearby superwinds have been discovered using optical imaging and spectroscopy to identify galaxy-sized outflows with velocities in excess of several hundred to a few thousand kilometers per second, and in most cases (e.g. M82 shown in Fig. 3) directly imaging structures aligned with the host galaxy’s transverse axis.

Because of the high prevalence of supernovae, starbursts should possess a large density of newly-born pulsars. Due to their important rotational and magnetic energy reservoirs these young neutron stars, with their metal-rich surfaces, have been explored as a potential engine for UHECR acceleration [72, 73]. The acceleration mechanism in a young neutron star is unipolar induction: In the out-flowing relativistic plasma, the combination of the fast star rotation and its strong magnetic field

⁶ Extragalactic magnetic fields may also be relevant for UHECR propagation in the intergalactic space; see e.g., [55].

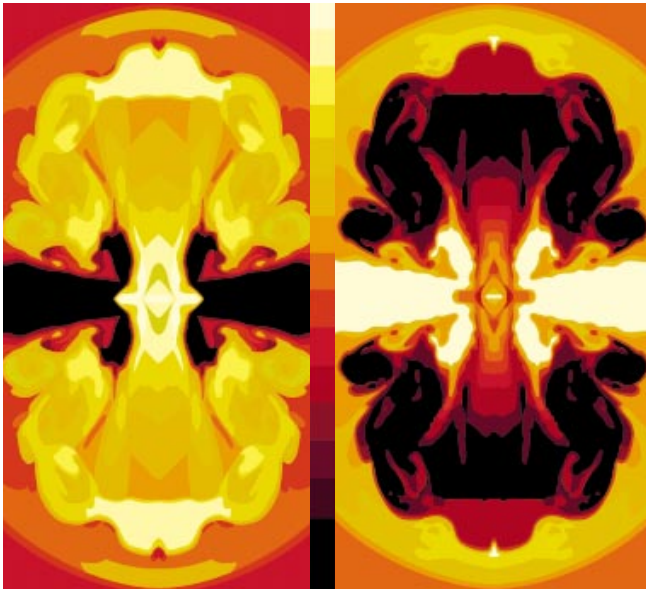


FIG. 2: Numerical simulation of a starburst's superwind. *Left panel.* Temperature map (bright = hot) showing how the hot gas emanating from the nucleus displaces the cooler galactic gas around it. *Right panel.* Gas density map (bright = dense) showing the inhomogeneous outflow along the rotation axis of the disk composed of a series of hot, dense, and fast shock fronts of material that are trailed by gas which has expanded, cooled, and slowed down. This figure is courtesy of Gerald Cecil [67].

can induce, in principle, potential differences of order $\Delta V = \Omega^2 \mu / c^2$, where $\mu = B_\star R_\star^3 / 2$ is the magnetic dipole moment, B is the surface dipole field strength, Ω is the rotation frequency, and $R_\star \sim 10$ km the star radius. The fastest spinning young neutron stars exhibit large magnetic fields typically in the range $10^{12} \lesssim B_\star / \text{G} \lesssim 10^{13}$, yielding $\mu \sim 10^{30.5}$ cgs. Provided that charged particles can experience a fraction η of that potential, they will be accelerated to the energy [72]

$$E(\Omega) = Ze \eta \Delta V \\ \sim 10^{11} \frac{Z}{26} \frac{\eta}{0.03} \left(\frac{\Omega}{10^4 \text{ s}^{-1}} \right)^2 \frac{\mu}{10^{30.5} \text{ cgs}} \text{ GeV}. \quad (8)$$

The fiducial value of Ω adopted in (8) corresponds to the exceptionally fast spinning young pulsars. The majority of pulsars are born spinning slower. Indeed, the distribution of pulsar-birth spin periods, $f(P = 2\pi/\Omega)$, is Gaussian, centered at 300 ms, with standard deviation of 150 ms [74]. Note that most of the pulsars would accelerate heavy nuclei up a few 10^6 GeV. Proto-pulsars spinning initially with $P \approx 6$ ms [75] could reach $E \sim 10^9$ GeV, which is roughly the maximum energy of Galactic cosmic rays [76].

Neutron-star surfaces are thought to be composed of anisotropic, tightly-bound condensed matter. The crust of neutron stars extends down to about 1 km below the surface, with densities ranging from a few g/cm^3 on the



FIG. 3: Telescopic snapshot of M82. Shortly after the identification of optical emission-line filaments [68] it became widely accepted that M82 is the archetype starburst galaxy [69]. The huge lanes of dust that crisscross the disk of M82 are the tell-tale signature of the flurry of star formation. Winds from massive stars and blasts from supernova explosions have created a strong superwind of galactic-scale, which is spewing knotty filaments of hydrogen and nitrogen gas [70, 71]. The red-glowing outwardly expanding filaments featuring the $\text{H}\alpha$ emission provide direct evidence for the galactic-scale superwind emanating from the central region to the outer halo area. This figure is courtesy of Leonardo Orazi.

exterior surface up to nuclear density $10^{14} \text{ g}/\text{cm}^3$ in the interior [77]. The outermost layers of a neutron stars are composed of iron. At densities $\gtrsim 10^4 \text{ g}/\text{cm}^3$, the atoms are fully ionized due to the pressure of the upper layers. The free electrons are degenerate and become relativistic at densities $> 10^6 \text{ g}/\text{cm}^3$. With increasing densities, the nuclei are more and more neutron rich owing to electron captures which convert protons into neutrons. This neutronization of the matter leads to the existence of a neutron ocean which permeates the inner layers of the crust at densities $\gtrsim 10^{11} \text{ g}/\text{cm}^3$. The crust dissolves into a uniform mixture of neutron, protons and electrons when the density reaches about $10^{14} \text{ g}/\text{cm}^3$. ^{56}Fe ions can thus be stripped off the surface and be accelerated through unipolar induction. A recent study [78] demonstrates that for the most reasonable range of neutron star surface temperatures ($T < 10^7$ K), a large fraction of nuclei survive *complete* photo-disintegration in the hostile environment sustained by the thermal radiation field from the star. However, the apparently inconsequential photo-disintegration losses could still be enough to produce a mixed nuclear composition at the source, with a non-negligible CNO component. The spectrum of accel-

erated UHECRs is determined by the evolution of the rotational frequency: As the star spins down, the energy of the ejected cosmic ray particles decreases. As a consequence, the total fluence of UHECRs accelerated in the neutron star magnetosphere is very hard, with spectrum $\propto E^{-1}$. Interestingly, as we noted in Sec. I, simultaneously reproducing Auger data on the spectrum together with the observed nuclear composition requires a hard source spectrum [22–24].

After the nuclei escape from the central region of the galaxy, with $10^6 \lesssim E/\text{GeV} \lesssim 10^9$, they are injected into the galactic-scale superwind and could potentially experience diffusive shock acceleration [79–83]. Diffusive shock acceleration is a first-order Fermi acceleration process [84] in which charged particles increase their energy by crossing the shock front multiple times, scattering off turbulence in the magnetic field B . The maximum achievable energy is obtained by setting the acceleration and flow time scales equal to each other [85]. The constraint due to the finite lifetime of the shock yields,

$$E_{\text{max}} \sim \frac{1}{12} Z e B v_{\text{sw}}^2 \tau, \quad (9)$$

where $v_{\text{sw}} \sim \sqrt{2\dot{E}_{\text{sw}}/\dot{M}_{\text{sw}}}$ is the asymptotic speed of the outflow in the superwind, \dot{E}_{sw} and \dot{M}_{sw} are respectively the energy and mass injection rates inside the spherical volume of the starburst region, and τ is the lifetime of the starburst, and where we have assumed a strong shock with a shock compression ratio $r = 8$ (associated to the adiabatic index of a polyatomic gas) [86]. In (9) it was implicitly assumed that the magnetic field is parallel to the shock normal. Injecting additional constraints into the model may reduce the maximum achievable energy [87, 88].

To get some idea of the orders of magnitude involved in (9), a very rough estimate can be made assuming M82 typifies the population of nearby starburst galaxies. The predicted kinetic energy and mass injection rates, derived from the measured IR luminosity, are $3 \times 10^{42} \text{ erg s}^{-1}$ and $3M_{\odot} \text{ yr}^{-1}$, respectively [62]. The gamma-ray, radio, and far infrared spectra of nearby starbursts seem to favor a synchrotron cooling timescale for electrons that is much shorter than their escape time [89]. It has been suggested that if electrons cool rapidly via synchrotron radiation, the magnetic energy density of the starburst region could be significantly higher than that expected from equipartition arguments with comparable cosmic rays and magnetic energy densities [90]. Indeed, if the magnetic energy density is in rough equipartition with its hydrostatic pressure, the implied magnetic field strength of M82 on few hundred parsec scales would be about 1.6 mG. Radio continuum and polarization observations provide an estimate of the magnetic field strength in the halo of M82, $B \sim 35 \mu\text{G}$ [91]. The age of the starburst phase is subject to large uncertainties. For our calculations, we adopt $\tau \sim 350 \text{ My}$, which is in the lower end of the average ages [92]. All in

all, substituting these figures into (9) we obtain

$$E_{\text{max}} \sim Z 10^{10} \text{ GeV}. \quad (10)$$

Note that (10) is consistent with the Hillas criterion [93], as the maximum energy of confined nuclei is found to be

$$E_{\text{max}} \simeq 10^9 Z \frac{B}{\mu\text{G}} \frac{R_{\text{sh}}}{\text{kpc}} \text{ GeV}, \quad (11)$$

where

$$R_{\text{sh}} \sim \sqrt{\frac{\dot{M}_{\text{sw}} v_{\text{sw}}}{2\Omega P_{\text{halo}}}} \sim 8 \text{ kpc} \quad (12)$$

is the shock radius, Ω is the solid angle subtended by the outflow cones, and P_{halo} is the pressure inside the halo [94]. In the estimate of (12) we have taken $\Omega \sim \pi$ and $P_{\text{halo}} \sim 10^{-14} \text{ erg cm}^{-3}$ [95]. The source emission spectrum would remain hard provided its shape is driven by UHECR nucleus leakage from the boundaries of the shock (a.k.a direct escape) [96]. Note that for $r = 8$, we expect a hard spectrum ($\propto E^{-1.4}$) at the sources [86].

The first generation of UHECR observatories reported several events above $10^{11.3} \text{ GeV}$, with no indication of a GZK cutoff. This would imply that if the UHECR were heavy nuclei, these sources must be nearby, less than about 3 Mpc away from Earth. More recent data, however, show a clear cutoff around $10^{10.6} \text{ GeV}$. These newer results then imply that UHECR nuclei could originate in more distant sources, as far away as about 50 Mpc, the canonical GZK horizon. The anisotropy study in [60] was based on data from first-generation observatories; newer data relax both the nuclear composition and the distance to sources.

An apparent correlation between UHECRs and nearby starbursts is visible in Fig. 4. As a matter of fact, the Pierre Auger Collaboration has recently reported an indication of a possible correlation between UHECRs ($E > 3.9 \times 10^{10} \text{ GeV}$) and starburst galaxies, with an *a posteriori* chance probability in an isotropic CR sky of $p_{\text{Auger}} = 4.2 \times 10^{-5}$, corresponding to a 1-sided Gaussian significance of 4σ [20, 21].⁷ In addition, the possible association of the TA hot spot with M82 has not gone unnoticed [98–100]. The multiplicative *p*-value for the two non-correlated observations is

$$p = p_{\text{TA}} \otimes p_{\text{Auger}} = 1.5 \times 10^{-8}, \quad (13)$$

yielding a statistical significance $\gtrsim 5\sigma$. However, caution must be exercised in all-sky comparisons [101]. Moreover, in (13) we have combined a catalog-based

⁷ Note that the significance of this *a posteriori* study does not account for the previous searches made within the Auger Collaboration and those made by others [20, 21].

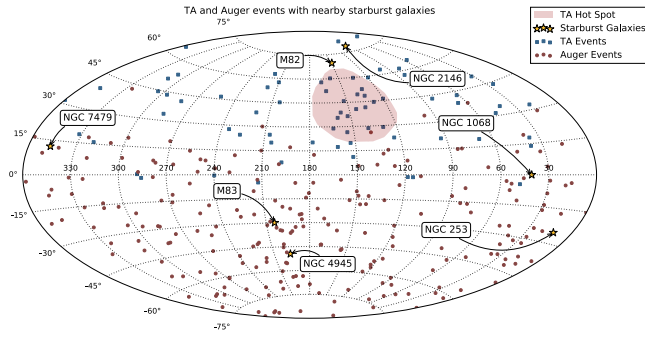


FIG. 4: Comparison of UHECR event locations with nearby starburst galaxies in equatorial coordinates, with R.A. increasing from right to left. The circles indicate the arrival directions of 231 events with $E > 52$ EeV and zenith angle $\theta < 80^\circ$ detected by the Pierre Auger Observatory from 2004 January 1 up to 2014 March 31 [97]. The squares indicate the arrival directions of 72 events with $E > 57$ EeV and $\theta < 55^\circ$ recorded from 2008 May 11 to 2013 May 4 with TA [18]. The stars indicate the location of nearby (distance < 50 Mpc) starburst galaxies. The shaded region delimits the TA hot-spot.

cross-correlated search (Auger) with a blind search (TA). Therefore, (13) provides a rough estimate of the statistical significance under the strong assumption that M82 (which is at the border of the excess of TA events) is the only source contributing to the TA hot spot. It is clear that new data are needed to confirm the suggested correlation. It is also clear that existing data concerning the distribution of arrival directions *do not rule out* the possibility of starbursts as UHECR emitters. Moreover, the hard emission spectrum from starburst galaxies renders them plausible candidate sources. Altogether, starbursts galaxies (shown in Fig. 1) emerge as the prominent example of source type.

We now turn to discuss how the joint study of anisotropy signals and nuclear composition could offer valuable clues for shedding light on nucleus-emitting-sources, such as starburst galaxies. A particularly interesting aspect of this study, which complements the likelihood fit proposed in Sec. II, is to analyze the pattern of anisotropies as a function of energy [102]. Note that if a source produces an anisotropy signal at energy E with cosmic ray nuclei of charge Ze , it should also produce a similar anisotropy pattern at energies E/Z via the proton component that is emitted along with the nuclei, given that the trajectory of cosmic rays within a magnetic field is only rigidity-dependent. Note that the central engine of the acceleration model discussed above is the neutron star surface, where iron nuclei are stripped off and can be accelerated to ultrahigh energies in a two-step process, without suffering catastrophic interactions. This means that the accompanying proton flux would be largely negligible. As noted in [103], secondary protons produced during propagation could also create an anisotropy pattern in the “low” energy regime. This sets a constraint on the maximum distance to nucleus-emitting-sources.

Making the extreme assumption that the source(s) responsible for TA and Auger anisotropies should lie closer than ~ 20 to 30 , 80 to 100 , and 180 to 200 Mpc, if the anisotropy signal is mainly composed of oxygen, silicon and iron nuclei, respectively [103]. We note that the starburst galaxies dominating the anisotropy signal are all at a distance $\lesssim 20$ Mpc, and consequently the model would also automatically satisfy this forceful constraint.

In regards to the expected *cepa stratis* structure introduced in Sec. III, we note that most UHECRs contributing to the possible correlation with starbursts (shown in Fig. 4) have energies below 10^{11} GeV. More specifically, in Table I we display the energy and arrival directions of UHECRs which are at $\lesssim 15^\circ$ degrees from our fiducial starburst galaxies. Only 3 out of the 44 events have energies in excess of 10^{11} GeV. The highest energy event, with $E \approx 1.3 \times 10^{11}$ GeV, appears to correlate with M83 which is only 4 Mpc away. The other two events are from sources which are beyond 15 Mpc, and from which we consequently expect species heavier than silicon; see Fig. 1. We conclude that there is a global agreement between the starburst hypothesis and data, interpreting these two events as a natural fluctuation.

Given that a strong evidence for a correlation between the arrival directions of UHECR and starbursts has been already established, the analysis method discussed in Sec. II should be adapted to this particular case. The multi-dimensional likelihood analysis to determine the source parameters and distance considering separate data from each cluster is still pending. This analysis would provide complementary information to test the starburst hypothesis of UHECRs. Predictions on possible mass composition can be advanced from Fig. 1, where we show distances to the nearest likely starburst galaxies. We see that there are four likely starburst candidates within 4 Mpc of Earth, and two more at ~ 15 Mpc from Earth. We get:

- the maximum average energy of nuclei arriving from NGC 2146 and/or NGC 1068 is roughly $10^{11.2}$ GeV;
- no ions lighter than ^{28}Si would be observed from NGC 2146 and/or NGC 1068 with an average energy beyond $10^{11.13}$ GeV;
- only nuclei lighter than neon, with a spectral cutoff $E \sim 10^{11}$ GeV, will appear to arrive from the direction (i.e. within 15° or so) of NGC 2146 and/or NGC 1068.

Another interesting application of our method is as follows. The sources NGC 1068 and NGC 7479 are located at about 15 and 35 Mpc, respectively. The propagation distances then engender specific patterns in the individual spectra and nuclear composition, e.g., no nuclear species lighter than ^{16}O would be expected above $E \sim 10^{10.9}$ GeV. Moreover, these two sources are located in a region of the sky in which the apertures of Auger and

TABLE I: Nearby starbursts, their location in the sky (SL), the CR energy ($E/(10^{10} \text{ GeV})$), the CR arrival direction (CR-AD), and the angular distance (δ) between SL and CR-AD for UHECRs which are within $\lesssim 15^\circ$ of the starbursts. If a given CR has two starbursts within 15° only the nearest source is given. SL and CR-AD are in equatorial coordinates (in degrees); δ is also given in degrees.

Starburst	SL	$E/(10^{10} \text{ GeV})$	CR-AD	δ
NGC 2146	(94.7, 78.4)	6.54	(87.6, 81.5)	3.4
NGC 2146	(94.7, 78.4)	6.42	(22.5, 80.1)	12.7
NGC 1068	(40.7, 0.0)	6.05	(47.7, -4.7)	8.2
NGC 1068	(40.7, 0.0)	6.69	(28.9, -2.7)	12.1
NGC 1068	(40.7, 0.0)	10.82	(45.6, -1.7)	5.2
NGC 1068	(40.7, 0.0)	6.77	(53.0, -4.5)	13.1
M82	(149.0, 69.7)	5.78	(158.6, 60.3)	10.2
M82	(149.0, 69.7)	7.69	(134.8, 59.8)	11.5
M82	(149.0, 69.7)	8.33	(168.5, 57.9)	14.4
NGC 7479	(346.2, 12.3)	6.52	(331.65, 18.85)	15.5
NGC 7479	(346.2, 12.3)	8.90	(349.9, 9.3)	4.7
NGC 7479	(346.2, 12.3)	5.67	(358.9, 15.5)	12.7
NGC 7479	(346.2, 12.3)	11.83	(340.6, 12.0)	5.5
NGC 253	(11.9, -25.3)	6.04	(19.8, -25.5)	12.4
NGC 253	(11.9, -25.3)	6.47	(15.6, -17.1)	12.7
NGC 253	(11.9, -25.3)	5.90	(26.7, -29.1)	13.6
NGC 253	(11.9, -25.3)	7.37	(12.3, -40.7)	15.4
NGC 253	(11.9, -25.3)	6.33	(26.1, -32.2)	14.2
NGC 253	(11.9, -25.3)	7.02	(4.6, -37.9)	14.0
NGC 253	(11.9, -25.3)	8.38	(26.8, -24.8)	13.5
NGC 253	(11.9, -25.3)	7.12	(17.5, -37.8)	13.4
NGC 4945	(196.4, -49.5)	5.86	(208.1, -60.1)	12.6
NGC 4945	(196.4, -49.5)	5.21	(199.1, -48.5)	2.0
NGC 4945	(196.4, -49.5)	6.95	(201.1, -55.3)	6.5
NGC 4945	(196.4, -49.5)	5.95	(200.9, -45.3)	5.2
NGC 4945	(196.4, -49.5)	6.00	(200.2, -43.4)	6.6
NGC 4945	(196.4, -49.5)	6.15	(219.5, -53.9)	14.9
NGC 4945	(196.4, -49.5)	6.19	(195.5, -63.4)	13.9
NGC 4945	(196.4, -49.5)	6.53	(187.5, -63.5)	14.8
NGC 4945	(196.4, -49.5)	5.33	(202.0, -54.9)	6.4
NGC 4945	(196.4, -49.5)	5.86	(217.9, -51.5)	13.8
M83	(204.2, -29.9)	5.92	(199.7, -34.9)	6.4
M83	(204.2, -29.9)	7.25	(193.8, -36.4)	10.9
M83	(204.2, -29.9)	12.71	(192.8, 21.2)	13.4
M83	(204.2, -29.9)	6.07	(192.5, -35.3)	11.3
M83	(204.2, -29.9)	5.81	(202.2, -16.1)	13.8
M83	(204.2, -29.9)	7.40	(209.6, -31.3)	4.8
M83	(204.2, -29.9)	6.67	(203.4, -33.0)	3.2
M83	(204.2, -29.9)	7.25	(193.8, -36.4)	10.9
M83	(204.2, -29.9)	5.47	(197.8, -20.0)	11.5
M83	(204.2, -29.9)	6.48	(207.1, -29.1)	2.6
M83	(204.2, -29.9)	5.57	(217.1, -24.5)	12.6
M83	(204.2, -29.9)	62.7	(200.9, -34.6)	5.5
M83	(204.2, -29.9)	7.45	(189.9, -32.7)	12.6

TA overlap. As a consequence, these sources can be used for normalization of the starburst hypothesis. Namely, even though the CR flux in the Northern and Southern skies may differ as a reflection of the cosmic variance, for a given angular aperture to the line-of-sight to these sources, the event rates should be the same for both Auger and TA. This is another concrete example of how the proposed multi-dimensional analysis could provide valuable clues to unmask the origin of UHECRs.

We note that other nearby starbursts may contribute to the UHECR flux observed on Earth, e.g., NGC 3079 at a distance of 16.2 Mpc is known to have a powerful large scale superwind [104, 105], and emission in the gamma ray band $0.1 < E/\text{GeV} < 100$ smaller than $2.2 \times 10^{-9} \text{ cm}^{-2} \text{ s}^{-1}$ [40]. The presence of these additional sources would not alter our conclusions.

Finally, we note that the starburst model has implications for ultrahigh energy neutrinos. As shown elsewhere [106], for very reasonable source parameters, we expect the radiation backgrounds to hardly disintegrate accelerated nuclei enabling a direct escape, largely without contributing to the cosmic neutrino flux. This is consistent with the emission of a negligible proton flux and the absence of anisotropy patterns at energies E/Z , in agreement with observations.

V. SUMMARY

It is well known that GZK interactions of UHECR nuclei *en route* to Earth favor heavy nuclei at the highest energies. The maximum energy of the acceleration capability of sources grows linearly in Z and hence also favors heavy nuclei at the highest energies. The traditional bi-dimensional analyses, which simultaneously reproduce Auger data on the spectrum and nuclear composition, may not be capable of distinguishing the relative importance of the two phenomena, and some kind of multi-dimensional analysis would be required. We have proposed a method for discriminating between these two end-of-energy models by reconstructing the individual emission spectra from various nearby sources.

We proposed to combine information on nuclear composition and arrival direction to associate a potential clustering of trans-GZK events with a 3-dimensional position in the sky. For a given cluster, the distance to the source and its maximum energy could be determined through a multi-parameter fit to the observed nuclear composition of each individual event, in conjunction with possible GZK energy losses. This allows for a model discrimination on an statistical basis by comparing the maximum energy at the source of each individual cluster.

We have identified a striking difference between the anisotropy patterns created by proton- and nucleus-emitting-sources. On the one hand, sources of UHECR nuclei display (after CR propagation) anisotropy patterns in the shape of onion layers, with radii that increase with rising energy. These hot spots are expected

to shine in the sky at energies $10^{10.6} \lesssim E/\text{GeV} \lesssim 10^{11}$. A prime example of sources of UHECR nuclei are starburst galaxies [30]. The Pierre Auger Collaboration has recently reported an indication of a possible correlation between CR with $E > 3.9 \times 10^{10}$ GeV and starburst galaxies, with an *a posteriori* significance level of 4σ [20, 21]. The smearing angle and the anisotropic fraction corresponding to the best-fit parameters are 13° and 10%. On the other hand, sources of UHECR protons display anisotropy patterns which become denser and compressed with rising energy. The Pierre Auger Collaboration has also reported a less significant (2.7σ) correlation between CR with $E > 6.0 \times 10^{10}$ GeV and the brightest radio loud active galactic nuclei (within a 250 Mpc radius from Earth) from the second catalog of hard *Fermi*-LAT sources [20, 21]. The smearing angle and the anisotropic fraction corresponding to the best-fit parameters are 7° and 7%. The high energy threshold and distinctively the smaller size of the hot spots may be indicative of UHECR protons. If this were the case these sources will be uncovered in the very near future. This is because the study of UHECRs with POEMMA will yield orders-of-magnitude increase in statistics of observed UHECRs, particularly beyond 10^{11} GeV where proton sources become unmistakable.

A point worth noting at this juncture is that albeit at first glance the analysis technique and conclusions presented herein may appear similar to those of [42], there are a few key differences which make the analyses complementary to one another. In [42] the authors consider all UHECR data with equal weights, and study the spectral shape fitting simultaneously both sub- and trans-GZK events. This study provides a general description of the observed UHECR spectrum, but ignores highly technical details of the nuclear composition at the high energy end of the spectrum. For example, the authors of [42] conclude that *light and intermediate (He, CNO and Si; respectively) mass nuclei are not expected to play any significant role above $\sim 10^{10.7}$ GeV due to their interaction with the photon backgrounds even if they were present or even dominant at the sources.* As we have shown in this paper, the multi-dimensional reconstruction of the individual trans-GZK spectra (in E , direction, and cross-correlation with nearby putative sources) highlights the importance of these nuclear species to uncover the *cepa stratis* structure portrayed by UHECR nucleus sources from our cosmic backyard.

We have also revisited the hypothesis that UHECR nuclei can originate in starburst galaxies. We have shown that iron nuclei can be stripped off the surface of young neutron stars (which are abundant in the central region of these galaxies) and can be accelerated without suffer-

ing catastrophic interactions in a two-step process that involves a one-shot acceleration in the potential drop of the fast-spinning pulsar, followed by re-acceleration at the large scale terminal shock produced by the superwind that flows from the starburst engine. The acceleration process yields a hard emission spectrum $\propto E^{-1}$, as needed to reproduce Auger data on both the spectrum and the observed nuclear composition. When the hard source spectrum is combined with the evidence for correlation we conclude that *starburst galaxies provide a compelling source example of UHECRs.* Using starbursts as a working example we demonstrated the functionality of the proposed multidimensional analysis.

In summary, we have demonstrated that our local universe encompasses a natural mass spectrometer that can be operated to untangle the origin of UHECRs. We have shown that while sources of nuclei design a *cepa stratis* structure in the sky, with the layer of the onion increasing with rising energy, proton accelerators imprint hot spots which become denser and compressed with rising energy. Future data from POEMMA [46] (and its pathfinder mission [107]), TA, and AugerPrime [45] will provide a final verdict for the ideas presented and discussed in this paper.

Dedication

We dedicate this work to the memory of Haim Goldberg (1939-2017). We cherish our long friendships and research with Haim. He was brilliant, but humble, always cheerful and thoughtful. He inspired us with his physics insights. The genesis of the idea explored here is a 2002 publication of Haim Goldberg, Diego Torres, and Luis Anchordoqui.

Acknowledgments

We would like to acknowledge many useful discussions with our colleagues of the Pierre Auger and POEMMA collaborations. We thank Gerald Cecil and Leonardo Orazi for permission to reproduce Figs. 2 and 3. LAA is supported by the U.S. National Science Foundation (NSF) Grant No. PHY-1620661 and by the National Aeronautics and Space Administration (NASA) Grant No. NNX13AH52G. VB is supported by the U. S. Department of Energy (DoE) Grant No. DE-FG-02-95ER40896. TJW is supported by DoE Grant No. DESC-0011981.

[1] R. U. Abbasi *et al.* [HiRes Collaboration], **First observation of the Greisen-Zatsepin-Kuzmin sup-**

pression, Phys. Rev. Lett. **100**, 101101 (2008) doi:10.1103/PhysRevLett.100.101101 [astro-ph/0703099].

- [2] J. Abraham *et al.* [Pierre Auger Collaboration], **Observation of the suppression of the flux of cosmic rays above 4×10^{19} eV**, Phys. Rev. Lett. **101**, 061101 (2008) doi:10.1103/PhysRevLett.101.061101 [arXiv:0806.4302 [astro-ph]].
- [3] T. Abu-Zayyad *et al.* [Telescope Array Collaboration], **The cosmic ray energy spectrum observed with the surface detector of the Telescope Array experiment**, Astrophys. J. **768**, L1 (2013) doi:10.1088/2041-8205/768/1/L1 [arXiv:1205.5067 [astro-ph.HE]].
- [4] J. N. Bahcall and E. Waxman, **Has the GZK cutoff been discovered?**, Phys. Lett. B **556**, 1 (2003) doi:10.1016/S0370-2693(03)00105-9 [hep-ph/0206217].
- [5] J. Abraham *et al.* [Pierre Auger Collaboration], **Measurement of the energy spectrum of cosmic rays above 10^{18} eV using the Pierre Auger Observatory**, Phys. Lett. B **685**, 239 (2010) doi:10.1016/j.physletb.2010.02.013 [arXiv:1002.1975 [astro-ph.HE]].
- [6] K. Greisen, **End to the cosmic ray spectrum?**, Phys. Rev. Lett. **16**, 748 (1966) doi:10.1103/PhysRevLett.16.748.
- [7] G. T. Zatsepin and V. A. Kuzmin, **Upper limit of the spectrum of cosmic rays**, JETP Lett. **4**, 78 (1966) [Pisma Zh. Eksp. Teor. Fiz. **4**, 114 (1966)].
- [8] R. Aloisio, V. Berezhinsky and A. Gazizov, **Ultra high energy cosmic rays: The disappointing model**, Astropart. Phys. **34**, 620 (2011) doi:10.1016/j.astropartphys.2010.12.008 [arXiv:0907.5194 [astro-ph.HE]].
- [9] J. L. Puget, F. W. Stecker and J. H. Bredekamp, **Photonuclear interactions of ultrahigh-energy cosmic rays and their astrophysical consequences**, Astrophys. J. **205**, 638 (1976). doi:10.1086/154321
- [10] L. Anchordoqui, M. T. Dova, A. G. Mariazzi, T. McCauley, T. C. Paul, S. Reucroft and J. Swain, **High energy physics in the atmosphere: Phenomenology of cosmic ray air showers**, Annals Phys. **314**, 145 (2004) doi:10.1016/j.aop.2004.07.003 [hep-ph/0407020].
- [11] J. Abraham *et al.* [Pierre Auger Collaboration], **Measurement of the depth of maximum of extensive air showers above 10^{18} eV**, Phys. Rev. Lett. **104**, 091101 (2010) doi:10.1103/PhysRevLett.104.091101 [arXiv:1002.0699 [astro-ph.HE]].
- [12] A. Aab *et al.* [Pierre Auger Collaboration], **Muons in air showers at the Pierre Auger Observatory: Measurement of atmospheric production depth**, Phys. Rev. D **90**, no. 1, 012012 (2014) Addendum: [Phys. Rev. D **90**, no. 3, 039904 (2014)] Erratum: [Phys. Rev. D **92**, no. 1, 019903 (2015)] doi:10.1103/PhysRevD.92.019903, 10.1103/PhysRevD.90.012012, 10.1103/PhysRevD.90.039904 [arXiv:1407.5919 [hep-ex]].
- [13] A. Aab *et al.* [Pierre Auger Collaboration], **Depth of maximum of air-shower profiles at the Pierre Auger Observatory I: Measurements at energies above $10^{17.8}$ eV**, Phys. Rev. D **90**, no. 12, 122005 (2014) doi:10.1103/PhysRevD.90.122005 [arXiv:1409.4809 [astro-ph.HE]].
- [14] A. Aab *et al.* [Pierre Auger Collaboration], **Depth of maximum of air-shower profiles at the Pierre Auger Observatory II: Composition implications**, Phys. Rev. D **90**, no. 12, 122006 (2014) doi:10.1103/PhysRevD.90.122006 [arXiv:1409.5083 [astro-ph.HE]].
- [15] A. Aab *et al.* [Pierre Auger Collaboration], **Evidence for a mixed mass composition at the “ankle” in the cosmic-ray spectrum**, Phys. Lett. B **762**, 288 (2016) doi:10.1016/j.physletb.2016.09.039 [arXiv:1609.08567 [astro-ph.HE]].
- [16] R. U. Abbasi *et al.*, **Study of ultrahigh energy cosmic ray composition using Telescope Arrays Middle Drum detector and surface array in hybrid mode**, Astropart. Phys. **64**, 49 (2014) doi:10.1016/j.astropartphys.2014.11.004 [arXiv:1408.1726 [astro-ph.HE]].
- [17] R. Abbasi *et al.* [Pierre Auger and Telescope Array Collaborations], **Report of the working group on the composition of ultrahigh energy cosmic rays**, arXiv:1503.07540 [astro-ph.HE].
- [18] R. U. Abbasi *et al.* [Telescope Array Collaboration], **Indications of intermediate-scale anisotropy of cosmic rays with energy greater than 57 EeV in the Northern sky measured with the surface detector of the Telescope Array experiment**, Astrophys. J. **790**, L21 (2014) doi:10.1088/2041-8205/790/2/L21 [arXiv:1404.5890 [astro-ph.HE]].
- [19] K. Kawata *et al.* [Telescope Array Collaboration], **Ultra-high-energy cosmic-ray hotspot observed with the Telescope Array surface detectors**, PoS ICRC **2015**, 276 (2016).
- [20] A. Aab *et al.* [Pierre Auger Collaboration], **The Pierre Auger Observatory: Contributions to the 35th International Cosmic Ray Conference (ICRC 2017)**, arXiv:1708.06592 [astro-ph.HE].
- [21] M. Unger *et al.* [Pierre Auger Collaboration], **Highlights from the Pierre Auger Observatory (ICRC17)**, PoS ICRC **2017**, 1102 (2017) [arXiv:1710.09478 [astro-ph.HE]].
- [22] R. Aloisio, V. Berezhinsky and P. Blasi, **Ultrahigh energy cosmic rays: implications of Auger data for source spectra and chemical composition**, JCAP **1410**, no. 10, 020 (2014) doi:10.1088/1475-7516/2014/10/020 [arXiv:1312.7459 [astro-ph.HE]].
- [23] M. Unger, G. R. Farrar and L. A. Anchordoqui, **Origin of the ankle in the ultrahigh energy cosmic ray spectrum, and of the extragalactic protons below it**, Phys. Rev. D **92**, no. 12, 123001 (2015) doi:10.1103/PhysRevD.92.123001 [arXiv:1505.02153 [astro-ph.HE]].
- [24] A. Aab *et al.* [Pierre Auger Collaboration], **Combined fit of spectrum and composition data as measured by the Pierre Auger Observatory**, JCAP **1704**, no. 04, 038 (2017) doi:10.1088/1475-7516/2017/04/038 [arXiv:1612.07155 [astro-ph.HE]].
- [25] A. M. Taylor, M. Ahlers and D. Hooper, **Indications of negative evolution for the sources of the highest energy cosmic rays**, Phys. Rev. D **92**, no. 6, 063011 (2015) doi:10.1103/PhysRevD.92.063011 [arXiv:1505.06090 [astro-ph.HE]].
- [26] M. Ahlers, L. A. Anchordoqui and A. M. Taylor, **Ensemble fluctuations of the flux and nuclear composition of ultrahigh energy cosmic ray nuclei**, Phys. Rev. D **87**, no. 2, 023004 (2013) doi:10.1103/PhysRevD.87.023004 [arXiv:1209.5427 [astro-ph.HE]].
- [27] L. A. Anchordoqui, M. Ahlers, A. V. Olinto, T. C. Paul and A. M. Taylor, **Sensitivity of JEM-EUSO to ensemble fluctuations in the ultrahigh energy cosmic ray flux**, arXiv:1306.0910 [astro-ph.CO].
- [28] A. M. Taylor, M. Ahlers and F. A. Aharonian, **The need for a local source of UHE CR nuclei**, Phys. Rev. D **84**, 105007 (2011) doi:10.1103/PhysRevD.84.105007 [arXiv:1107.2055 [astro-ph.HE]].
- [29] S. R. Coleman and S. L. Glashow, **High-energy tests of Lorentz invariance**, Phys. Rev. D **59**, 116008 (1999) doi:10.1103/PhysRevD.59.116008 [hep-ph/9812418].
- [30] L. A. Anchordoqui, G. E. Romero and J. A. Combi, **Heavy**

- nuclei at the end of the cosmic ray spectrum?, Phys. Rev. D **60**, 103001 (1999) doi:10.1103/PhysRevD.60.103001 [astro-ph/9903145].
- [31] G. R. Blumenthal, **Energy loss of high-energy cosmic rays in pair-producing collisions with ambient photons**, Phys. Rev. D **1**, 1596 (1970). doi:10.1103/PhysRevD.1.1596
- [32] F. A. Aharonian and J. W. Cronin, **Influence of the universal microwave background radiation on the extragalactic cosmic ray spectrum**, Phys. Rev. D **50**, 1892 (1994). doi:10.1103/PhysRevD.50.1892
- [33] M. J. Chodorowski, A. A. Zdziarski, and M. Sikora, **Reaction rate and energy-loss rate for photopair production by relativistic nuclei**, Astrophys. J. **400**, 181 (1992). doi:10.1086/171984
- [34] F. W. Stecker, **Photo-disintegration of ultrahigh-energy cosmic rays by the universal radiation field**, Phys. Rev. **180**, 1264 (1969). doi:10.1103/PhysRev.180.1264
- [35] S. Karakula and W. Tkaczyk, **Astropart. Phys.** **1**, 229 (1993). doi:10.1016/0927-6505(93)90023-7
- [36] L. A. Anchordoqui, J. F. Beacom, H. Goldberg, S. Palomares-Ruiz and T. J. Weiler, **TeV gamma-rays from photo-disintegration/de-excitation of cosmic-ray nuclei**, Phys. Rev. Lett. **98**, 121101 (2007) doi:10.1103/PhysRevLett.98.121101 [astro-ph/0611580].
- [37] L. N. Epele and E. Roulet, **On the propagation of the highest energy cosmic ray nuclei**, JHEP **9810**, 009 (1998) doi:10.1088/1126-6708/1998/10/009 [astro-ph/9808104].
- [38] A. Dominguez *et al.*, **Extragalactic background light inferred from AEGIS galaxy SED-type fractions**, Mon. Not. Roy. Astron. Soc. **410**, 2556 (2011) doi:10.1111/j.1365-2966.2010.17631.x [arXiv:1007.1459 [astro-ph.CO]].
- [39] R. C. Gilmore, R. S. Somerville, J. R. Primack and A. Dominguez, **Semi-analytic modeling of the EBL and consequences for extragalactic gamma-ray spectra**, Mon. Not. Roy. Astron. Soc. **422**, 3189 (2012) doi:10.1111/j.1365-2966.2012.20841.x [arXiv:1104.0671 [astro-ph.CO]].
- [40] M. Ackermann *et al.* [Fermi-LAT Collaboration], **GeV observations of star-forming galaxies with Fermi-LAT**, Astrophys. J. **755**, 164 (2012) doi:10.1088/0004-637X/755/2/164 [arXiv:1206.1346 [astro-ph.HE]].
- [41] D. J. Bird *et al.*, **Detection of a cosmic ray with measured energy well beyond the expected spectral cutoff due to cosmic microwave radiation**, Astrophys. J. **441**, 144 (1995) doi:10.1086/175344 [astro-ph/9410067].
- [42] D. Allard, N. G. Busca, G. Decerprit, A. V. Olinto and E. Parizot, **Implications of the cosmic ray spectrum for the mass composition at the highest energies**, JCAP **0810**, 033 (2008) doi:10.1088/1475-7516/2008/10/033 [arXiv:0805.4779 [astro-ph]].
- [43] D. Allard, **Extragalactic propagation of ultrahigh energy cosmic-rays**, Astropart. Phys. **39-40**, 33 (2012) doi:10.1016/j.astropartphys.2011.10.011 [arXiv:1111.3290 [astro-ph.HE]].
- [44] S. Wykes, A. M. Taylor, J. D. Bray, M. J. Hardcastle and M. Hillas, **UHECR propagation from Centaurus A**, arXiv:1706.08229 [astro-ph.HE].
- [45] A. Aab *et al.* [Pierre Auger Collaboration], **The Pierre Auger Observatory Upgrade - Preliminary Design Report**, arXiv:1604.03637 [astro-ph.IM].
- [46] A. V. Olinto *et al.*, **POEMMA: Probe Of Extreme Multi-Messenger Astrophysics**, PoS ICRC **2017**, 542 (2017) [arXiv:1708.07599 [astro-ph.IM]].
- [47] A. Aab *et al.* [Pierre Auger Collaboration], **Inferences on mass composition and tests of hadronic interactions from 0.3 to 100 EeV using the water-Cherenkov detectors of the Pierre Auger Observatory**, Phys. Rev. D (to be published) [arXiv:1710.07249 [astro-ph.HE]].
- [48] M. S. Pshirkov, P. G. Tinyakov, P. P. Kronberg and K. J. Newton-McGee, **Deriving global structure of the Galactic magnetic field from Faraday rotation measures of extragalactic sources**, Astrophys. J. **738**, 192 (2011) doi:10.1088/0004-637X/738/2/192 [arXiv:1103.0814 [astro-ph.GA]].
- [49] R. Jansson and G. R. Farrar, **A new model of the Galactic magnetic field**, Astrophys. J. **757**, 14 (2012) doi:10.1088/0004-637X/757/1/14 [arXiv:1204.3662 [astro-ph.GA]].
- [50] R. Jansson and G. R. Farrar, **The Galactic magnetic field**, Astrophys. J. **761**, L11 (2012) doi:10.1088/2041-8205/761/1/L11 [arXiv:1210.7820 [astro-ph.GA]].
- [51] M. Unger and G. R. Farrar, **Uncertainties in the magnetic field of the Milky Way**, arXiv:1707.02339 [astro-ph.GA].
- [52] G. R. Farrar, **The Galactic magnetic field and ultrahigh-energy cosmic ray deflections**, Comptes Rendus Physique **15**, 339 (2014) doi:10.1016/j.crhy.2014.04.002 [arXiv:1405.3680 [astro-ph.HE]].
- [53] A. Aab *et al.* [The Pierre Auger Collaboration], **Observation of a large-scale anisotropy in the arrival directions of cosmic rays above 8×10^{18} eV**, Science **357**, 1266 (2017) doi:10.1126/science.aan4338 [arXiv:1709.07321 [astro-ph.HE]].
- [54] G. R. Farrar and M. S. Sutherland, **Deflections of UHECRs in the Galactic magnetic field**, arXiv:1711.02730 [astro-ph.HE].
- [55] A. van Vliet, R. Alves Batista and G. Sigl, **Extragalactic sources and propagation of UHECRs**, arXiv:1705.02293 [astro-ph.HE].
- [56] D. F. Torres and L. A. Anchordoqui, **Astrophysical origins of ultrahigh energy cosmic rays**, Rept. Prog. Phys. **67**, 1663 (2004) doi:10.1088/0034-4885/67/9/R03 [astro-ph/0402371].
- [57] N. Hayashida *et al.*, **Observation of a very energetic cosmic ray well beyond the predicted 2.7-K cutoff in the primary energy spectrum**, Phys. Rev. Lett. **73**, 3491 (1994). doi:10.1103/PhysRevLett.73.3491
- [58] M. Takeda *et al.*, **Extension of the cosmic ray energy spectrum beyond the predicted Greisen-Zatsepin-Kuz'min cutoff**, Phys. Rev. Lett. **81**, 1163 (1998) doi:10.1103/PhysRevLett.81.1163 [astro-ph/9807193].
- [59] S. P. Knurenko, Z. E. Petrov and I. S. Petrov, **Radio emission of air showers with extremely high energy measured by the Yakutsk radio array**, doi:10.1016/j.nima.2017.04.033 arXiv:1705.01260 [astro-ph.IM].
- [60] L. A. Anchordoqui, H. Goldberg and D. F. Torres, **Anisotropy at the end of the cosmic ray spectrum?**, Phys. Rev. D **67**, 123006 (2003) doi:10.1103/PhysRevD.67.123006 [astro-ph/0209546].
- [61] S. Veilleux, G. Cecil and J. Bland-Hawthorn, **Galactic winds**, Ann. Rev. Astron. Astrophys. **43**, 769 (2005) doi:10.1146/annurev.astro.43.072103.150610 [astro-ph/0504435].
- [62] T. M. Heckman and T. A. Thompson, **A brief review of galactic winds** arXiv:1701.09062.
- [63] G. H. Rieke, M. J. Lebofsky, R. I. Thompson, F. J. Low and A. T. Tokunaga, **The nature of the nuclear sources in M82 and NGC 253**, Astrophys. J. **238**, 24 (1980). doi:10.1086/157954

- [64] T. M. Heckman, L. Armus and G. K. Miley, *On the nature and implications of starburst-driven galactic superwinds*, *Astrophys. J. Suppl.* **74**, 833 (1990). doi:10.1086/191522
- [65] R. A. Chevalier and A. W. Clegg, *Wind from a starburst galaxy nucleus*, *Nature* **317**, 44 (1985). doi:10.1038/317044a0
- [66] C. G. Hoopes, T. M. Heckman, D. K. Strickland and J. C. Howk, *Cooling in coronal gas in the M82 starburst superwind*, *Astrophys. J.* **596**, L175 (2003) doi:10.1086/379533 [astro-ph/0309245].
- [67] S. Veilleux, G. Cecil, and J. Bland-Hawthorn, *Colossal galactic explosions* *Sci. Am.* **17**, 50 (2007) doi:10.1038/scientificamerican0407-50sp
- [68] C. R. Lynds and A. R. Sandage *Evidence for an explosion in the center of the galaxy M82* *Astrophys. J.* **137**, 1005 (1963).
- [69] R. W. O’Connell and J. J. Mangano, *The central regions of M82* *Astrophys. J.* **221**, 62 (1978).
- [70] A. A. Suchkov, V. G. Berman, T. M. Heckman, and D. S. Balsara *Mass loading and collimation of galactic superwinds* *Astrophys. J.* **463**, 528 (1996).
- [71] P. L. Shopbell and J. Bland-Hawthorn, *The asymmetric wind in M82*, *Astrophys. J.* **493**, 129 (1998) doi:10.1086/305108 [astro-ph/9708038].
- [72] P. Blasi, R. I. Epstein and A. V. Olinto, *Ultrahigh-energy cosmic rays from young neutron star winds*, *Astrophys. J.* **533**, L123 (2000) doi:10.1086/312626 [astro-ph/9912240].
- [73] K. Fang, K. Kotera and A. V. Olinto, *Newly-born pulsars as sources of ultrahigh energy cosmic rays*, *Astrophys. J.* **750**, 118 (2012) doi:10.1088/0004-637X/750/2/118 [arXiv:1201.5197 [astro-ph.HE]].
- [74] C. A. Faucher-Giguere and V. M. Kaspi, *Birth and evolution of isolated radio pulsars*, *Astrophys. J.* **643**, 332 (2006) doi:10.1086/501516 [astro-ph/0512585].
- [75] P. Haensel, J. P. Lasota and J. L. Zdunik, *On the minimum period of uniformly rotating neutron stars*, *Astron. Astrophys.* **344**, 151 (1999) [astro-ph/9901118].
- [76] K. Fang, K. Kotera and A. V. Olinto, *Ultrahigh energy cosmic ray nuclei from extragalactic pulsars and the effect of their Galactic counterparts*, *JCAP* **1303**, 010 (2013) doi:10.1088/1475-7516/2013/03/010 [arXiv:1302.4482 [astro-ph.HE]].
- [77] N. Chamel and P. Haensel, *Physics of neutron star crusts*, *Living Rev. Rel.* **11**, 10 (2008) doi:10.12942/lrr-2008-10 [arXiv:0812.3955 [astro-ph]].
- [78] K. Kotera, E. Amato and P. Blasi, *The fate of ultrahigh energy nuclei in the immediate environment of young fast-rotating pulsars*, *JCAP* **1508**, no. 08, 026 (2015) doi:10.1088/1475-7516/2015/08/026 [arXiv:1503.07907 [astro-ph.HE]].
- [79] A. R. Bell, *The acceleration of cosmic rays in shock fronts I*, *Mon. Not. Roy. Astron. Soc.* **182**, 147 (1978).
- [80] A. R. Bell, *The acceleration of cosmic rays in shock fronts II*, *Mon. Not. Roy. Astron. Soc.* **182**, 443 (1978).
- [81] P. O. Lagage and C. J. Cesarsky, *The maximum energy of cosmic rays accelerated by supernova shocks*, *Astron. Astrophys.* **125**, 249 (1983).
- [82] L. O. Drury, *An introduction to the theory of diffusive shock acceleration of energetic particles in tenuous plasmas*, *Rept. Prog. Phys.* **46**, 973 (1983). doi:10.1088/0034-4885/46/8/002
- [83] R. Blandford and D. Eichler, *Particle acceleration at astrophysical shocks: A theory of cosmic ray origin*, *Phys. Rept.* **154**, 1 (1987). doi:10.1016/0370-1573(87)90134-7
- [84] E. Fermi, *On the origin of the cosmic radiation*, *Phys. Rev.* **75**, 1169 (1949). doi:10.1103/PhysRev.75.1169
- [85] T. K. Gaisser, *Cosmic rays and particle physics*, (Cambridge University Press, UK, 1990)
- [86] L. A. Anchordoqui, *Ultrahigh-energy cosmic ray acceleration in starburst superwinds*, in preparation.
- [87] E. G. Zweibel, *Cosmic ray history and its implications for galactic magnetic fields*, *Astrophys. J.* **587**, 625 (2003) doi:10.1086/368256 [astro-ph/0212559].
- [88] C. Bustard, E. G. Zweibel and C. Cotter, *Cosmic ray acceleration by a versatile family of galactic wind termination shocks*, *Astrophys. J.* **835**, no. 1, 72 (2017) doi:10.3847/1538-4357/835/1/72 [arXiv:1610.06565 [astro-ph.HE]].
- [89] T. A. D. Paglione and R. D. Abrahams, *Properties of nearby starburst galaxies based on their diffuse gamma-ray emission*, *Astrophys. J.* **755**, 106 (2012) [arXiv:1206.3530 [astro-ph.HE]].
- [90] T. A. Thompson, E. Quataert, E. Waxman, N. Murray and C. L. Martin, *Magnetic fields in starburst galaxies and the origin of the fir-radio correlation*, *Astrophys. J.* **645**, 186 (2006) [astro-ph/0601626].
- [91] M. Krause, *Magnetic fields and halos in spiral galaxies*, arXiv:1401.1317 [astro-ph.GA].
- [92] K. B. W. McQuinn *et al.*, *The nature of starbursts II: The duration of starbursts in dwarf galaxies*, *Astrophys. J.* **724**, 49 (2010) doi:10.1088/0004-637X/724/1/49 [arXiv:1009.2940 [astro-ph.CO]].
- [93] A. M. Hillas, *The origin of ultrahigh-energy cosmic rays*, *Ann. Rev. Astron. Astrophys.* **22**, 425 (1984). doi:10.1146/annurev.aa.22.090184.002233
- [94] B. C. Lacki, *The Fermi Bubbles as starburst wind termination shocks*, *Mon. Not. Roy. Astron. Soc.* **444**, L39 (2014) doi:10.1093/mnras/slu107 [arXiv:1304.6137 [astro-ph.HE]].
- [95] A. Shukurov, G. R. Sarson, A. Nordlund, B. Gudiksen and A. Brandenburg, *The effects of spiral arms on the multi-phase ISM*, *Astrophys. Space Sci.* **289**, 319 (2004) doi:10.1023/B:ASTR.0000014960.35780.2e [astro-ph/0212260].
- [96] P. Baerwald, M. Bustamante and W. Winter, *UHECR escape mechanisms for protons and neutrons from GRBs, and the cosmic ray-neutrino connection*, *Astrophys. J.* **768**, 186 (2013) doi:10.1088/0004-637X/768/2/186 [arXiv:1301.6163 [astro-ph.HE]].
- [97] A. Aab *et al.* [Pierre Auger Collaboration], *Searches for anisotropies in the arrival directions of the highest energy cosmic rays detected by the Pierre Auger Observatory*, *Astrophys. J.* **804**, no. 1, 15 (2015) doi:10.1088/0004-637X/804/1/15 [arXiv:1411.6111 [astro-ph.HE]].
- [98] L. A. Anchordoqui, T. C. Paul, L. H. M. da Silva, D. F. Torres and B. J. Vlcek, *What IceCube data tell us about neutrino emission from star-forming galaxies (so far)*, *Phys. Rev. D* **89**, no. 12, 127304 (2014) doi:10.1103/PhysRevD.89.127304 [arXiv:1405.7648 [astro-ph.HE]].
- [99] H. N. He, A. Kusenko, S. Nagataki, B. B. Zhang, R. Z. Yang and Y. Z. Fan, *Monte Carlo Bayesian search for the plausible source of the Telescope Array hot spot*, *Phys. Rev. D* **93**, 043011 (2016) doi:10.1103/PhysRevD.93.043011 [arXiv:1411.5273 [astro-ph.HE]].
- [100] D. N. Pfeffer, E. D. Kovetz and M. Kamionkowski,

- Ultra-high-energy-cosmic-ray hot spots from tidal disruption events, *Mon. Not. Roy. Astron. Soc.* **466**, 2922 (2017) doi:10.1093/mnras/stw3337 [arXiv:1512.04959 [astro-ph.HE]].
- [101] N. Globus, D. Allard, E. Parizot, C. Lachaud and T. Piran, *Can we reconcile the TA excess and hotspot with Auger observations?*, *Astrophys. J.* **836**, no. 2, 163 (2017) doi:10.3847/1538-4357/836/2/163 [arXiv:1610.05319 [astro-ph.HE]].
- [102] M. Lemoine and E. Waxman, *Anisotropy vs chemical composition at ultra-high energies*, *JCAP* **0911**, 009 (2009) doi:10.1088/1475-7516/2009/11/009 [arXiv:0907.1354 [astro-ph.HE]].
- [103] R. Y. Liu, A. M. Taylor, M. Lemoine, X. Y. Wang and E. Waxman, *Constraints on the source of ultra-high-energy cosmic rays using anisotropy versus chemical composition*, *Astrophys. J.* **776**, 88 (2013) doi:10.1088/0004-637X/776/2/88 [arXiv:1308.5699 [astro-ph.HE]].
- [104] G. Cecil, J. Bland-Hawthorn, S. Veilleux and A. V. Filippenko, *Jet- and wind-driven ionized outflows in the superbubble and star-forming disk of NGC 3079*, *Astrophys. J.* **555**, 338 (2001) doi:10.1086/321481 [astro-ph/0101010].
- [105] G. Cecil, J. Bland-Hawthorn and S. Veilleux, *Tightly correlated x-ray/H-alpha emitting filaments in the superbubble and large scale superwind of NGC 3079*, *Astrophys. J.* **576**, 745 (2002) doi:10.1086/341861 [astro-ph/0205508].
- [106] L. A. Anchordoqui, D. Hooper, S. Sarkar and A. M. Taylor, *High-energy neutrinos from astrophysical accelerators of cosmic ray nuclei*, *Astropart. Phys.* **29**, 1 (2008) doi:10.1016/j.astropartphys.2007.10.006 [astro-ph/0703001].
- [107] J. H. Adams *et al.*, *White paper on EUSO-SPB2*, arXiv:1703.04513 [astro-ph.HE].